Pak Heart J 2023:56(02)
ISSN:0048-2706 E-ISSN:2227-9199

DFT studies of electronic properties, molecular descriptors and partition coefficients of tautomers of favipiravir: a potential drug for the treatment of COVID-19

Chuol Ket Monyjok[1], Bang Chuol Nhial[2], G. Y. Sagar[3], N. Surendra Babu[4]
[1]Assistant Professor, Department of Environmental Science, College of Agriculture and Natural Resources, Gambella University, Ethiopia
[2]Lecturer, Department of Public Health, College of Natural and Computational Sciences, Gambella University, Ethiopia
[3]Professor, Department of Statistics, College of Natural and Computational Sciences, Gambella University, Ethiopia
[4]Computational Quantum Chemistry Lab, Department of Chemistry, College of Natural & Mathematical Sciences, University of Dodoma, Dodoma, Tanzania

Corresponding Author:
nsbabusk@gmail.com

ABSTRACT
Computational quantum research was conducted for structural analysis of Favipiravir and its behaviour against COVID-19. Favipiravir customers were studied first of all and found to be regarded as ligands by four tautomeric structures. All calculations are performed in calculations of density functional theory (DFT). Conducted molecular docking simulations were allocated to similar protease and polymerase macromolecules in COVID-19. The utility of the descriptor values for global reactivity to predict the reactivity of the favipiravir tautomers has been determined by HOMO and LUMO energies. Compared to others, the FA tautomer exhibits a lower value, and one can assume that it is more likely that FA will participate in electrophile reactions than other tautomers at any stage. The operation of amide-form favipiravir has a higher binding affinity with 6LU7 in the overall docking procedure compared to the other tautomer forms. The results showed that the four ligands would interact differently with each target. FK is the most stable, and FE is the most active macromolecular ligand. It has been found that ligands are not so strongly linked to the low values of connecting energies. The action of ligands is more favourable to protease than to polymeras a target. Qualitative ligand...target interaction representations have suggested various interaction environments with complex formations. Further research is also required to investigate Favipiravir's dominant activities against COVID-19.

Keywords: Favipiravir, COVID-19, tautomers, global descriptors, DFT method and Docking.

Introduction

Favipiravir ($C_5H_4FN_3O_2$, 6-fluoro-3-hydroxy-2-pyrazine carboxamide) is an antiviral medication based on pyrazinecarboxamides that is effective against a variety of viral infectious diseases, including influenza viruses (types A, B, and C),[1] H5N1 virus,[2] hepatotropic phleboviral diseases,[3]West Nile virus,[4] Norwalk virus (norovirus),[5]encephalitis viruses,[6] arenaviruses,[7] bunnyvirus[7] and Ebola virus.[8,9] As a result, Favipiravir sold under Avigan is considered an antiviral in large-scale agent, which inhibits the reproduction of viral infections of ribonucleic acid (RNA).[10] First Toyama Chemical Co., Ltd, Japan, registered Favipiravir in 2000.[11] Differing investigators made significant efforts to alter, optimize and improve cost-efficient and straightforward routes for favipiravir synthesis due to its effective antiviral potency.[12–15] Favipiravir has been examined as one of the possible medicines for the experimental treatment of new coronavirus disease as a consequence of the latest outbreak of the novel coronavirus disease 2019 (COVID-19), an infectious disease due to the severe acute coronavirustwo disease (SARS-CoV-2) in the world.[16–26]Favipiravir RTP is a polymerase RNA inhibitor that prevents transcriptions and replication of viral RNA-dependent polymerase.[27] Various hypotheses were developed about how favipiravir RTP interacts with RNA-dependent RNA polymerase, which demonstrates that it is incorporated into an emerging RNA strand preventing the elongation of the RNA strand and viral proliferation.[28] The existence of purine nucleoside analogs is likely to considerably reduce the antiviral activity of FPV, indicating a rivalry for the same binding site between FPV and the purine nucleosides. Most preclinical data of favipiravir are associated with influenza and Ebola but have shown widespread activity compared with other RNA viruses.[28]It is identified that Favipiravir has in vitro activity against SARS-CoV-2, although with high chloroquine or remdesivir concentrations (EC_{50} = 61.88 μM).[29]

Even though favipiravir and Ebola virus have a similar high EC_{50}, it has been shown in previous animal models to be highly successful as post-exposure prophylaxis for mice exposed to Ebola virus challenges, with rapid virological responses preventing mortality.[8,30] Human Ebola trials were conducted on a loading regimen of 6000

mg per day followed by 1200 mg per day orally for 10 days in a singlearm, and two different people produced results: It successfully weakened the Ebola for 10 in Guinea, but it did not affect its overall patient survival.[31]In a study of 124 Ebola virus patients in Sierra Leone, those given favipiravir had a significantly higher survival rate than those given supportive care (56.4 percent versus 35.3 percent; P = 0.027).[32] On day 1, patients were given 800 mg of favipiravir orally twice daily, and on day 2, they received 800 mg of favipiravir orally twice daily. On days 3–11, take 600 mg twice a day orally. In addition, the viral loads of 35 patients were measured twice during their hospitalization and were found to be significantly lower in those who received favipiravir.

A systemic investigation was conducted to examine the structural properties of Favipiravir tautomers. The chemical structures of favipiravir and its tautomers are provided in Figure 1. In cyclic compounds,[33-36] conformational modifications of Favipiravir could also undergo ubiquitous tautomerism processes. Moreover, these molecules may have keto-enol tautomerism that may be of interest to the design and production of drug products to decide which tautomeric forms are bound to a targeted bio-molecule. However, no theory of the conformational analysis, electronic and reactivity descriptors and partition coefficients of favipiravir and its structural analogs are carried out systematically and comparativelybecause of the significant applications of favipiravir.

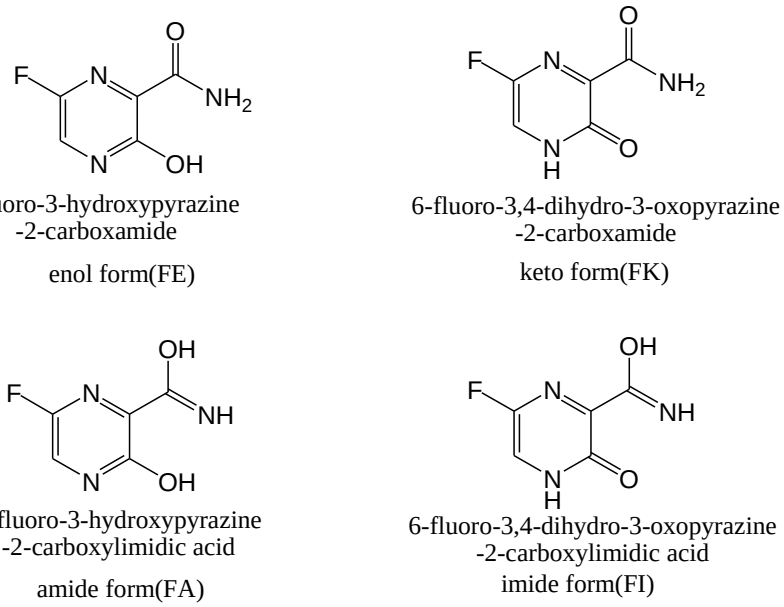

Figure 1. The tautomeric structures of Favipiravir are represented based on the H atom movement.

Structures of all Favipiravir tautomeric types have been studied on the grounds of quantum chemistry computations, and then molecular docking simulations of associated protease and polymerase to COVID-19 have been studied for their biological function. Note that silicon environments could offer computations of molecular scales to provide insight into the complex interaction complexes of the ligand.[37-41] Such studies will help explain the molecular structures, electronic characteristics and descriptors, and favipiravir partitions coefficients used to develop new antiviral drugs based on pyrazinecarboxamide.

Materials and method

Computational Details

The Gaussian 09W suite of programs[42] has been used to perform all quantum chemical calculations for the tautomers of Favipiravir (fig:1). Geometry optimizations for all tautomers have been performed using density functional theory (DFT) at the B3LYP functional[43–45] in conjunction with the 6-311G basis set. To characterize their existence as minimum or transition states and correct energies for zero-point energy and thermal contribution, we performed a harmonical measurement of the strength at each stationary point. The Gaussveiw software[46] extracted electrostatic potential maps (EPM). Polarizable Continuum Model (PCM),[47] as implemented in Gaussian 09W, describes solvent effects.

Molecular Docking simulations

Protein and Ligand Preparations

For the current study, the crystal structure of the COVID -19 protease enzyme was collected from the Protein data bank (rcsb.org)[48] with PDB ID 6LU7. The 6LU7 structure was prepared by energy minimization and coordinated

interaction sites using SWISS-PDB viewer[49] and Discovery studio client (BIOVIA, Dassault Systems)[50] of the PDB file, followed by saving a required format for further analysis. The structure of favipiravir was acquired from a drug bank;[51] using ChemDraw,[52] the tautomeric designs were drawn and checked the structural integrity with the help of an inbuilt suite in the software, followed by saving the required formats including .mol and .sdf formats.

Docking Executions

Auto dock 4.0 and Auto dock tools are more versatile for preparing the docking environment with standard protocol management,[53-55,] which includes a set of parameters to assign for the receptor grid in the ligand-binding coordinates and ligand acquisition for the docking. Once the auto dock environment is ready, using the standard configuration file and Microsoft cmd prompt, auto dock Vina is executed for recording the values for the binding affinity of the ligands towards the receptor, as mentioned above**.** After completing the docking procedure with auto dock Vina, the saved file formats are viewed with Discovery studio client and PyMol software[56] to analyze ligand receptors' affinity with 2D and 3D illustration objects.

Results and discussion

Structural parameters

The DFT method with B3LYP functional and 6-311G basis set was performed in gas and different solvents without symmetry restriction and convergence criteria for geometry optimization for favipiravir and tautomers. Figure 2 shows a minimum energy geometry and atomic numeration. Table 1 shows the bond lengths and selected bond angles of the optimized structure of FE in gas and different solvents. Tables S1-S3 provided the geometrical parameters of the remaining tautomers (FA,FE and FI).

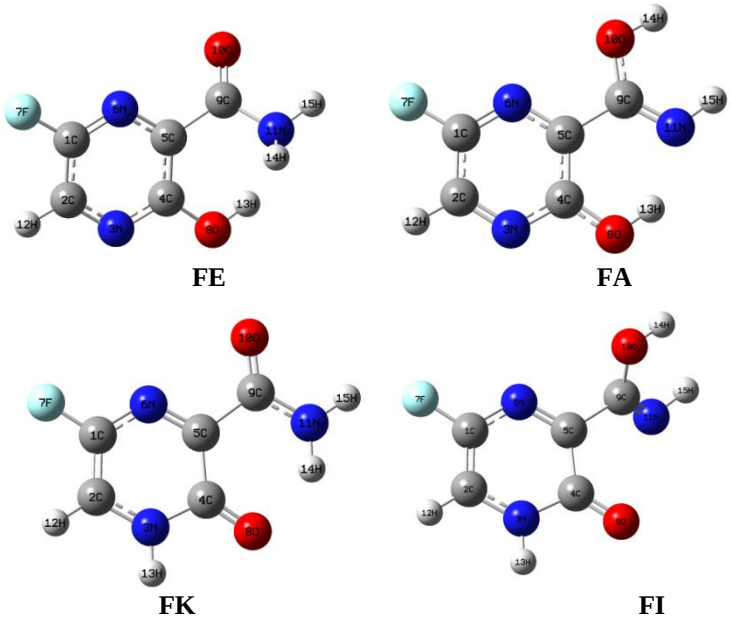

Figure 2. Geometry optimization structures of favipiravir and its structural tautomers at DFT/B3LYP/6-311G basis set in the gas phase.

Table 1, together with the experimental values for FE, provides the bond lengths and selective bond angles of the optimized structures of tautomers. The structural parameters calculated for FE are compatible with the experimental values. For the bond length and the endocylic bond angles in the pyrazine ring, the correlation (R^2) between the experimental and theoretical values is determined to be 0.9677. (Figure 3)

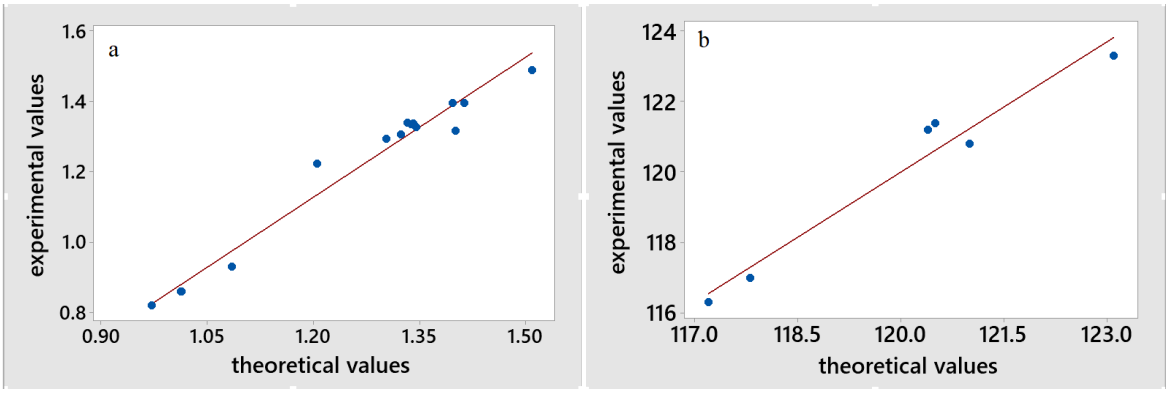

Figure 3. Correlation between the experimental and theoretical values of FE tautomer.

Table.1: Some of the selected optimized structural parameters for favipiravir (FE tautomer) in gas and different solvents at DFT/B3LYP/6-311G level.

Bond length					
Parameter[a]	**Expt[b]**	**Gas**	**water**	**octanol**	**Hexane**
1C-2C	1.397	1.397	1.394	1.395	1.396
1C-6N	1.295	1.303	1.303	1.303	1.303
1C-7F	1.339	1.341	1.345	1.344	1.342
2C-3N	1.306	1.324	1.326	1.326	1.325
2C-12H	0.930	1.085	1.084	1.084	1.085
N3-4C	1.340	1.333	1.334	1.334	1.334
C4-5C	1.397	1.414	1.412	1.413	1.413
C4-8O	1.328	1.346	1.345	1.345	1.346
C5-6N	1.335	1.338	1.338	1.338	1.338
C5-9C	1.489	1.509	1.509	1.509	1.509
O8-13H	0.820	0.972	0.973	0.973	0.973
C9-10O	1.224	1.205	1.215	1.213	1.209
C9-11N	1.318	1.401	1.378	1.381	1.392
N11-14H	0.860	1.014	1.013	1.013	1.013
N11-15H	0.860	1.013	1.013	1.013	1.013
Bond angles					
2C-1C-6N	123.3	123.1	123.4	123.3	123.2
1C-2C-3N	121.2	120.4	120.0	120.0	120.2
2C-3N-4C	117.0	117.8	118.0	118.0	117.8
3N-4C-5C	120.8	121.0	121.1	121.1	121.0
4C-5C-6N	121.4	120.5	120.2	120.3	120.4
1C-6N-5C	116.3	117.2	117.4	117.3	117.3

[a]The atom numbering is given in Figure 2.
[b]Experimental values for T705 compounds taken from reference [13].

2.2 Relative stabilities

The overall and relative energies (at level DFT/6-311G) of four favipiravir tautomers are presented in Table 2, four two are keto-enol tautomers (FE and FE) and two are amide-imide tautomers (FA and FI). The most stable tautomer FK is considered a reference when calculating relative energies for tautomers. Results suggest that the two amino and imide are of the highest energy among four tautomers since hydrogen atoms can migrate and the simultaneous transfers a little more than atoms can be eliminated. Still, the hydrogen atom can only be exchanged in a very similar and distinct way between heteroatoms by more than two atoms. Relative stability order of tautomers in the gas phase is: FK> FE > FI>FA. At equilibrium, the enol form predominates. For this series of tautomers, however, the enol form is strongly favoured by the aromatic nature of the keto ring. The intramolecular hydrogen connection between the hydrogen atom and the oxygen atom of the carbonyl group is also stabilizing the enol form.

Table 2. The energies of tautomers(a.u) at DFT/B3LYP/6-311G level in gas and different solvents and the relative energies compared to the most stable isomer FK. The relative energies in brackets in kcal mol^{-1}.

Tautomer	Gas	Water	Octanol	Hexane
FE	-607.647351	-607.664692	-607.662085	-607.653792
	(4.66)	**(7.13)**	**(6.80)**	**(5.65)**
FA	-604.319471	-604.335910	-604.333515	-604.325686
	(2092.90)	**(2095.94)**	**(2095.48)**	**(2095.04)**
FK	-607.654783	-607.676047	-607.672929	-607.662800
	(0.00)	(0.00)	(0.00)	(0.00)
FI	-607.617665	-607.640827	-607.637266	-607.626091
	(23.29)	**(22.10)**	**(22.38)**	**(23.03)**

Solvent effects are essential in phenomena of stability of tautomers because polarity differences between tautomers can lead to significant changes in their relative solvent energies. The solvent effects for favipiravir tautomerism were analyzed using SCRF/B3LYP calculations. The relative energies in Table 1 show that polar solvents increase all favipiravir tautomers' stability compared to the gas phase. When changing from the gas phase to the solvent phase, the total energy of Favipiravir and tautomers shows no regular pattern. The interactions of solvents have marked the level of stability in the gasphase of the tautomers.

2.3 The Thermodynamic Parameters

Entropy, enthalpy, heat capacity, exceptional heat capacity, and many more are essential thermodynamic properties of solids. Molecular stability, binding features of biologically active protein molecules, and physicochemical properties are analyzed using thermodynamic properties.[57-59]Table 3 contains the thermodynamic parameters in various mediums; the ΔH, ΔG and ΔS values are suitable for different solvents, except $FK \rightarrow FI$ that the negative value is in gas and $FK \rightarrow FA$ negative values in solvents of water and octanol. The change of enthalpies (ΔH) values are all positive, i.e. endothermic reaction, ΔS usually is relatively small (in cal/mole in table 3) to compare to other thermodynamic properties (ΔH and ΔG), indicating that with no ring formation or other unusual changes in the constraints between the products and reactants.

Table 3. The enthalpy (ΔH), Gibbs free energy (ΔG) values in kcal/mol and entropy(ΔS) in cal/mol Kelvin, and equilibrium constants for the tautomers at DFT/6-311G level in the gas phase and different solvents

Gas **Tautomer equilibrium**	**ΔH**	**ΔG**	**ΔS**	**K**	p_T^K
$FK \rightarrow FE$	4.63	5.00	12.55	2.16 $X10^{-17}$	3.66
$FK \rightarrow FA$	2097.75	2099.05	60.87	0.00	0.00
$FK \rightarrow FI$	22.87	22.05	-61.49	6.84 $X10^{-17}$	16.16
Water					
$FK \rightarrow FE$	7.00	34.80	8.16	3.07 $X10^{-26}$	25.51
$FK \rightarrow FA$	2100.51	2101.58	-28.87	0.00	0.00
$FK \rightarrow FI$	21.81	21.13	38.28	3.23 $X10^{-16}$	15.49
Octanol					
$FK \rightarrow FE$	6.70	6.84	479.41	9.67 $X10^{-6}$	5.01
$FK \rightarrow FA$	2100.03	2101.15	-38.28	0.00	0.00
$FK \rightarrow FI$	22.08	21.76	272.33	1.12 $X10^{-16}$	15.95
Hexane					
$FK \rightarrow FE$	5.58	5.89	1521.69	4.81 $X10^{-5}$	4.31
$FK \rightarrow FA$	2098.76	2099.94	721.63	0.00	0.00
$FK \rightarrow FI$	22.68	22.17	668.29	5.58 $X10^{-17}$	16.25

2.4 Equilibrium Constants

We determined their tautomeric equilibrium constants with the relation's help to determine the changes in kinetic parameters.[60]

$$K_T = e^{-\frac{\Delta G}{RT}} \quad (1)$$

K_T is the equilibrium constant;the gas constant R is $1.987x10^{-3}$ kcal/mol, and T is 298.15 k. The amount ΔG is the difference in stable energy between the Gibbs free energy of the tautomer. From equation[61,] the p_T^K values of the tautomer were calculated concerning stable tautomer FE. Table 3 included equilibrium values (K), gas, and different solvents determined from the most stable tautomer FE. All values in the gas phase and the two solvents were positive, confirming the stability of FE Tautomer. All gases and solvents with a pK^T value of 3.66, 25.51, 5.01 and 4.31 for gas, water, octanol and hexane calculated equilibrium levels between favipiravir tautomers indicate that the FK is dominant over the FE. The FK type is more prevalent than the FA and FI shape.

2.5 HOMO-LUMO energy gap (ΔE_g)

Table 4 in the gas phase and various solvents summarizes the HOMO, LUMO and HOMO- LUMO gapenergies. Figures 4 and 5 display the 3D plots for the highest molecular orbital (HOMO) and the lowest molecular orbital (LUMO) of favipiravir and its tautomers. These plots are generated from optimized and frequency calculations. The HOMO orbitals are distributed over the entire molecules, whereas the pyrazine ring and the carboxamide group are placed in the LUMO orbital, as shown in the figure.

In terms of chemical stability, HOMO and LUMO energies are involved. The HOMO is the power to donate an electron, while LUMO represents the capacity to absorb an electron as an electron receiver. The HOMO's energy is directly linked to the ionizationpotential, and LUMO's energy directly correlates with the electron's affinity. The high value of HOMO energy can show that the molecule is inclined to give electrons to an accepting molecule of low, empty, orbital molecules. Conversely, electron acceptance is more likely due to the lower values of LUMO energy. Thus, the energy gap (ΔE_g) is an effective stability indicator, namely the difference in energy between the HOMO and LUMO. The wider the energy differences between LUMO and HOMO, the easier they are to excite the HOMO electrons; the higher the HOMO energies, the easier they are to give electrons; the lower the LUMO energies, the easier the electrons can be accepted by the molecules. From Figure 6, the amide form (FA) ΔE_g is high value at all phases.

Table 4. The global descriptors calculated by DFT/6-311 in the gas phase and different solvents

Medium	**Gas**				**Water**			
Molecule	**FE**	**FA**	**FK**	**FI**	**FE**	**FA**	**FK**	**FI**
HOMO	-7.23252	-9.2712	-6.96557	-6.53727	-7.1615	-9.31854	-6.78435	-6.54761
LUMO	-2.45637	-1.55432	-2.89638	-2.45719	-2.36739	-1.53908	-2.75651	-2.57474
ΔE_g	4.77614	7.71688	4.06919	4.08008	9.52889	7.77947	4.02783	3.97286
I	7.23252	9.2712	6.96557	6.53727	-7.1615	9.31854	6.78435	6.54761
A	2.45637	1.55432	2.89638	2.45719	2.36739	1.53908	2.75651	2.57474
X	4.84445	5.41276	4.93098	4.49723	-2.39705	5.42881	4.77043	4.56117
H	2.38807	3.85844	2.0346	2.04004	-4.76444	3.88973	2.01392	1.98643
M	-4.84445	-5.41276	-4.93098	-4.49723	2.39705	-5.42881	-4.77043	-4.56117
S	0.41875	0.25917	0.4915	0.49019	-0.20989	0.25709	0.49655	0.50342
Ω	4.91372	3.7966	5.97527	4.95703	-0.60299	3.78843	5.64994	5.2366
ΔN_{max}	2.0286	1.40284	2.42357	2.20448	0.50311	1.39568	2.36873	2.29616
ΔE_n	2.45735	2.24229	3.07889	2.49984	-2.97039	2.24936	2.89343	2.66186
ΔE_e	12.14624	13.0678	12.94085	11.4943	-7.76449	13.10698	12.43429	11.78421
Medium	**octane**				**Hexane**			
Molecule	**FE**	**FA**	**FK**	**FI**	**FE**	**FA**	**FK**	**FI**
HOMO	-7.17129	-9.31256	-6.80884	-6.54108	-7.17129	-9.29024	-6.89238	-6.534
LUMO	-2.37746	-1.54289	-2.77311	-2.57474	-2.37746	-1.5535	-2.83543	-2.48603

ΔE_g	4.79383	7.76967	4.03572	3.96633	4.79383	7.73675	4.05695	4.04797
I	7.17129	9.31256	6.80884	6.54108	7.17129	9.29024	6.89238	6.534
A	2.37746	1.54289	2.77311	2.57474	2.37746	1.5535	2.83543	2.48603
X	4.77438	5.42772	4.79098	4.55791	4.77438	5.42187	4.8639	4.51002
H	2.39692	3.88484	2.01786	1.98317	2.39692	3.86837	2.02847	2.02398
M	-4.77438	-5.42772	-4.79098	-4.55791	-4.77438	-5.42187	-4.8639	-4.51002
S	0.4172	0.25741	0.49557	0.50424	0.4172	0.25851	0.49298	0.49408
Ω	4.755	3.79169	5.68757	5.23772	4.755	3.79962	5.83136	5.02481
ΔN_{max}	1.99188	1.39716	2.37428	2.2983	1.99188	1.40159	2.39781	2.22829
ΔE_n	2.37754	2.2488	2.91445	2.66298	2.37754	2.24612	2.99594	2.53877
ΔE_e	11.92629	13.10424	12.4964	11.77879	11.92629	13.08986	12.72374	11.55881

Indeed, the solvent effects of HOMO and LUMO energies must be studied, and the number of solvents linked to these orbitals and thus chemical reactivity tested. The dielectric constant of solvent is increasing, the energy difference between HOMO and LUMO grows, and tautomers are more stable due to the significant (E_{HOMO}-E_{LUMO}) compounds. The Figure 6 readings show the order of stability in all phases of tautomers is identical

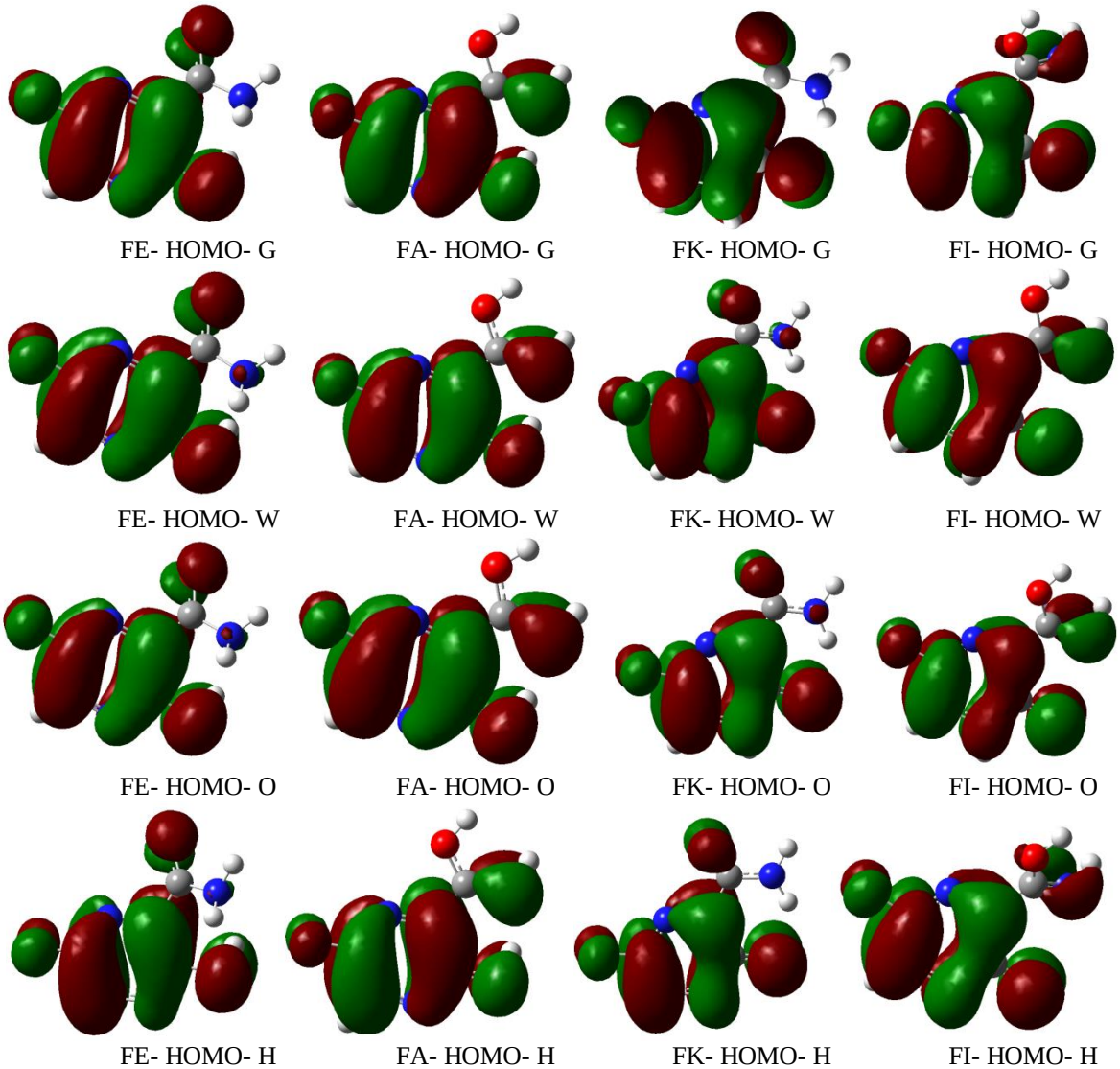

FE- HOMO- G FA- HOMO- G FK- HOMO- G FI- HOMO- G

FE- HOMO- W FA- HOMO- W FK- HOMO- W FI- HOMO- W

FE- HOMO- O FA- HOMO- O FK- HOMO- O FI- HOMO- O

FE- HOMO- H FA- HOMO- H FK- HOMO- H FI- HOMO- H

Figure 4. Highest occupied molecular orbitals (HOMO) for favipiravir and its tautomers at DFT/B3LYP/-311G basis set in gas (O), water (W), octanol (O) and hexane (H).

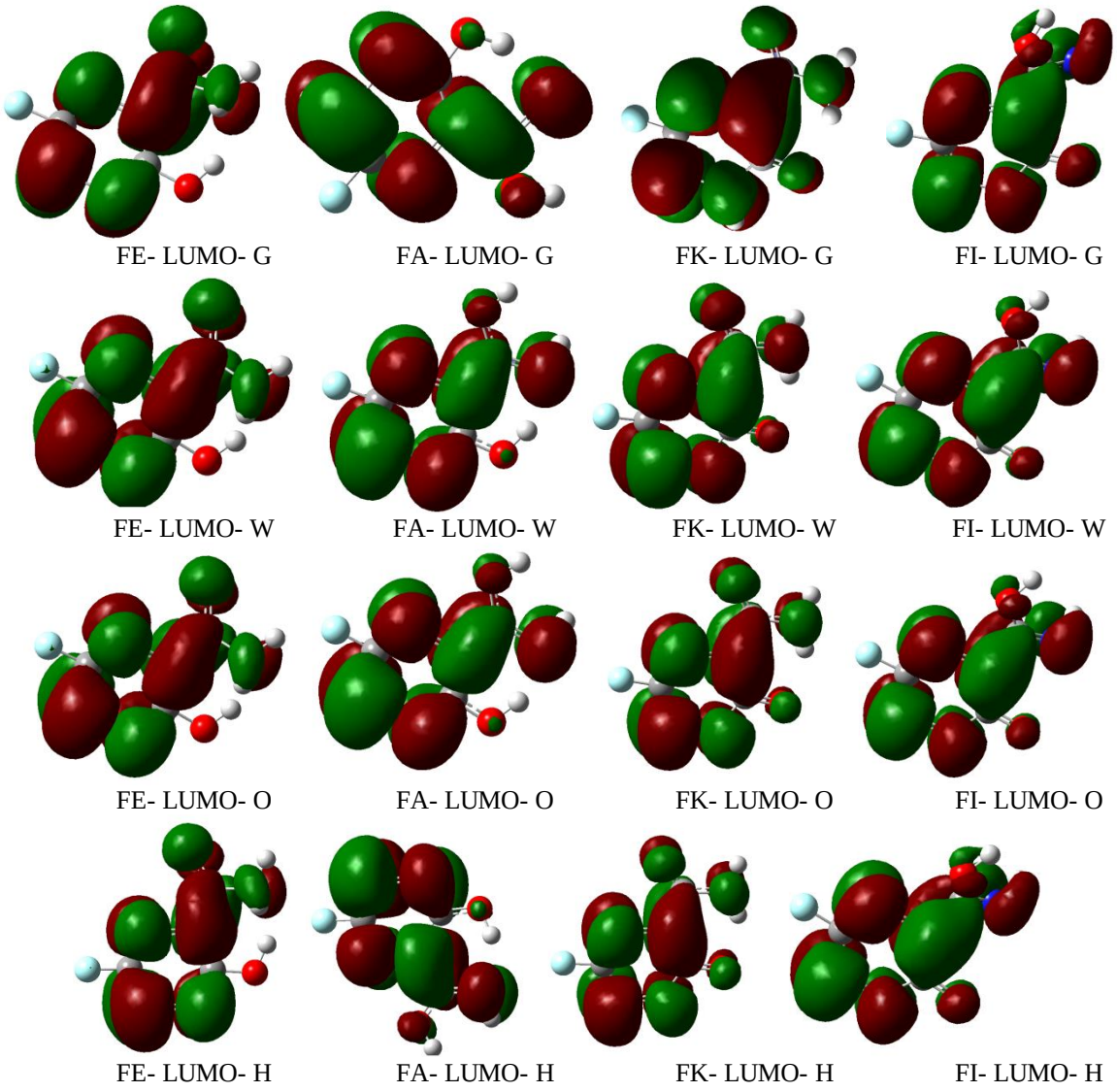

Figure 5. Lowest occupied molecular orbitals (HOMO) for favipiravir and its tautomers at DFT/B3LYP/-311G basis set in gas (O), water (W), octanol (O) and hexane (H).

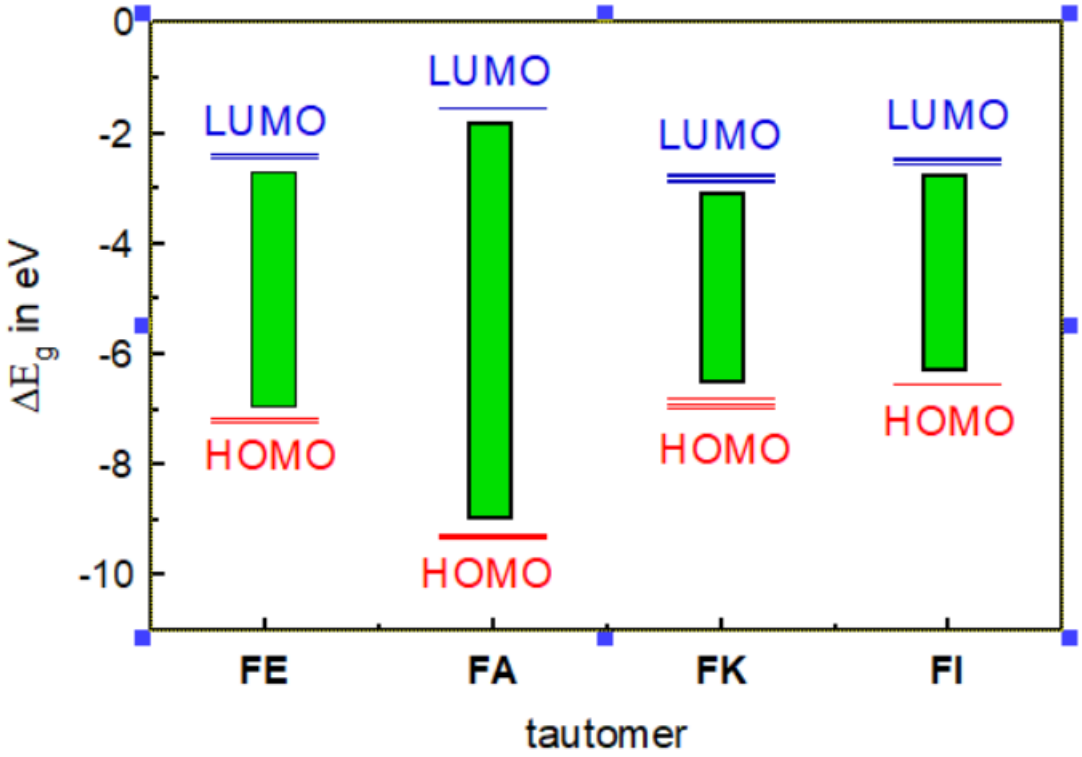

Figure 6. The calculated HOMO –LUMO energy gap Vs the studied tautomers in gas and different solvents.

2.6 Quantum chemical molecular descriptors:

Quantum chemical parameters arise from the measurements of molecular structures with various quantum mechanical outputs. These equations derive from the electronic interactions of the component atoms and thus refer mainly to their intrinsic characteristics. Many QSAR studies have used molecular descriptors measured using quantum mechanical methods.[62]As the reaction species regulate several chemical reactions, the most well-known quantum chemical descriptors are HOMO and LUMO energies.[63] In terms of HOMO and LUMO; you can also clearly describe the definition of hard and soft nucleophiles, electrophiles and molecule stability, and active durability. Some molecular descriptors most used for QSPR analytical applications are molecular orbital energy sources like HOMO, LUMO etc. and their derived numerical values like HOMO-LUMO energy gap, ionizing potential (IP), the affinity of electrons (EA), electron-negativity (χ), hardness (η), hardness (S), chemical potentials(μ), electrophilicity index (ω).[64,65] The calculated molecular descriptors of favipiravir tautomers are presented in Table 4 in gas and different solvents. The global descriptors are calculated by using the following equations

$$\chi = -\frac{(E_{HOMO} + E_{LUMO})}{2} = \frac{I + A}{2} \quad (2)$$

$$\mu = \frac{(E_{HOMO} + E_{LUMO})}{2} \quad (3)$$

$$\eta = \frac{E_{LUMO} - E_{HOMO}}{2} \quad (4)$$

$$s = \frac{1}{2\eta} \quad (5)$$

$$\omega = \frac{\mu^2}{2\eta} \quad (6)$$

Ayers and coworkers[66] proposed two new reactivity indices for quantifying the ability of nucleophiles and electrophiles to quit the community, nucleofugality (ΔE_n) and electrofugality (ΔE_e), which are explained as follows:

$$\Delta E_n = -A + \omega = \frac{(\mu + \eta)^2}{2\eta} \quad (7)$$

$$\Delta E_e = I + \omega = \frac{(\mu - \eta)^2}{2\eta} \quad (8)$$

The electrophilicity index was used as a structural descriptor for the chemical reactivity study of molecules. Compared to others, the calculated value for the FA tautomer is lower; one may assume that the FA would have a better tendency to participate in electrophile reactions than other tautomers at any point. Chemical potential (μ) defines the trend to escape from a balance system of electrons.

2.7 Partition coefficients

Partition coefficients are used in various solvent conditions to verify the accuracy of the atomic force fields. The concentration ratios for a neutral solvent molecule in a system of two immiscible solvents are clarified.

$$P = \frac{[solute]_{Organic}}{[solute]_{Aqueous}} \quad (9)$$

Where solute is a neutral solvent, the concentration ratio of either solvent is typically stated as a logarithm P (logP).[67]

This is different from the "apparent partition coefficient," which covers the solution's ionized and unionized forms.[68] Log P is proportional to the free energy transfer between the two solvents and can be related to free solvent energies. Solvency-free sources were used to measure[69–71] and notify changes[72] to fields of nuclear strength, including the force field GROMOS 53A5, which was partially parametrized using solvency-free enthalpies in cyclohexane.[73] The following are: However, solvent-free energies can be compared to partition coefficients which are relatively simple to calculate and regularly measure.[74]The Council of Europe Partition coefficients report is an excellent way to measure and enhance the accuracy of atomic force fields in various solvent environments due to experimental logP values and their direct connection to solvent-free energy.

As these values are common in the pharmaceutical industry, several tools exist to forecast the partitioning of octanol and water coefficients ($logP_{oct}$). In the pharmaceutical industry, partitioning coefficients are used to estimate how a drug can move among biological environments and are routinely used to predict the hydrophobicity of a molecule. Also, several methods use log P_{oct} as a measured input parameter for the quantitative structure-activity relationship (QSAR).[74]

Table. 5: Calculated solvation free energy change of transfer from the gas phase to water phase ($\Delta G_{solv(water)}$ / kcal mol^{-1}) and octanol phase ($\Delta G_{solv(octanol)}$ / kcal mol^{-1}) under standard state conditions, and corresponding logP values of examined B3LYP/6-311 level of theory.

	$\Delta G_{sol.\ w}$	$\Delta G_{sol.\ o}$	$\Delta G_{o/w}$	Log p
FE	-10.44	16.66	27.10	19.8704
FA	-15.16	-10.61	4.55	3.3382
FK	-9.15	-13.14	-3.99	-2.9233
FI	-9.66	-14.07	-4.41	-3.2307

The SMD solvation model was applied to four tautomers of favipiravir with B3LYP 6-311G as a basic set. Frequency calculations for all gas phase, water, and octanol molecules have been performed for geometry optimizations. Table 5 shows the partition coefficients. LogP is used in the pharmaceutical/biotech industry to explain the function of the drug molecules in the body. Drug candidates will also be tested for directing the LogP pharmaceutical selection and analogueoptimization. This is because lipophilicity determines the absorbent body distribution, penetration through essential membranes, and the biological obstacles of a compound (ADME properties). The compound designed for oral administration should be logP < 5 following 'Lipinski's rules of 5' (developed at Pfizer)

More fatty: poorly soluble and bio disposable. If the drug cannot achieve or keep sufficient concentration, the most potent in-vitro product cannot be effective.In addition, the fatty tissue can be sequestered and challenging to excrete; it adds to the buildup, causing systemic toxicity. It might not be feasible to create such obstacles. Ideal CNS-oriented medicinal products should have a logP value of about two[75] while a sub-sorption drug should have a logP value of > 5; oral and intestinal absorption is outstanding at 1.35–1.8. The low coefficient of octanol and water split, mainly seen inthe body's fluid, is characterized by a specific matter.[76] Table5 shows that FI (low for log P= -3.2307) is highly hydrophilic, and FE is very lipophilic (high for log P=19.8704).

2.8 Atomic Mulliken charges (AMCs)

The B3LYP/6-311G equilibrium geometric structures using the Gaussian09 were used to measure the atomic Mulliken charges. Tables S4-S7 provided Mulliken charges of tautomers. In Figure 7, gas and various solvents

demonstrate atomic charges of FE along with three other structural analogs. The distribution of charges is identical for all molecules, but the magnitude of the charges differs slightly. N3, N6, O10 and N11 and O8 molecules are negatively loaded since the electronegativity of the atoms are considerably higher than the carbon and hydrogen atoms. Possibly charged, but with the electron withdrawal effect of adjacentO8, hydroxyl H13 is more optimistic. The carboxamide group's H14 and H15 hydrogen atoms and carbonyl carbon atom C9 are charged with a nearly equivalent magnitude for all molecules. The pyrazine rings C2, C4 and C5 are positive, but the hydroxyl O8 influences C4 more positively. The atomic charges of 0.3136e for FA, 0.4113e for FK, 0.02774e for FI, 0.2659e for FI, respectively.

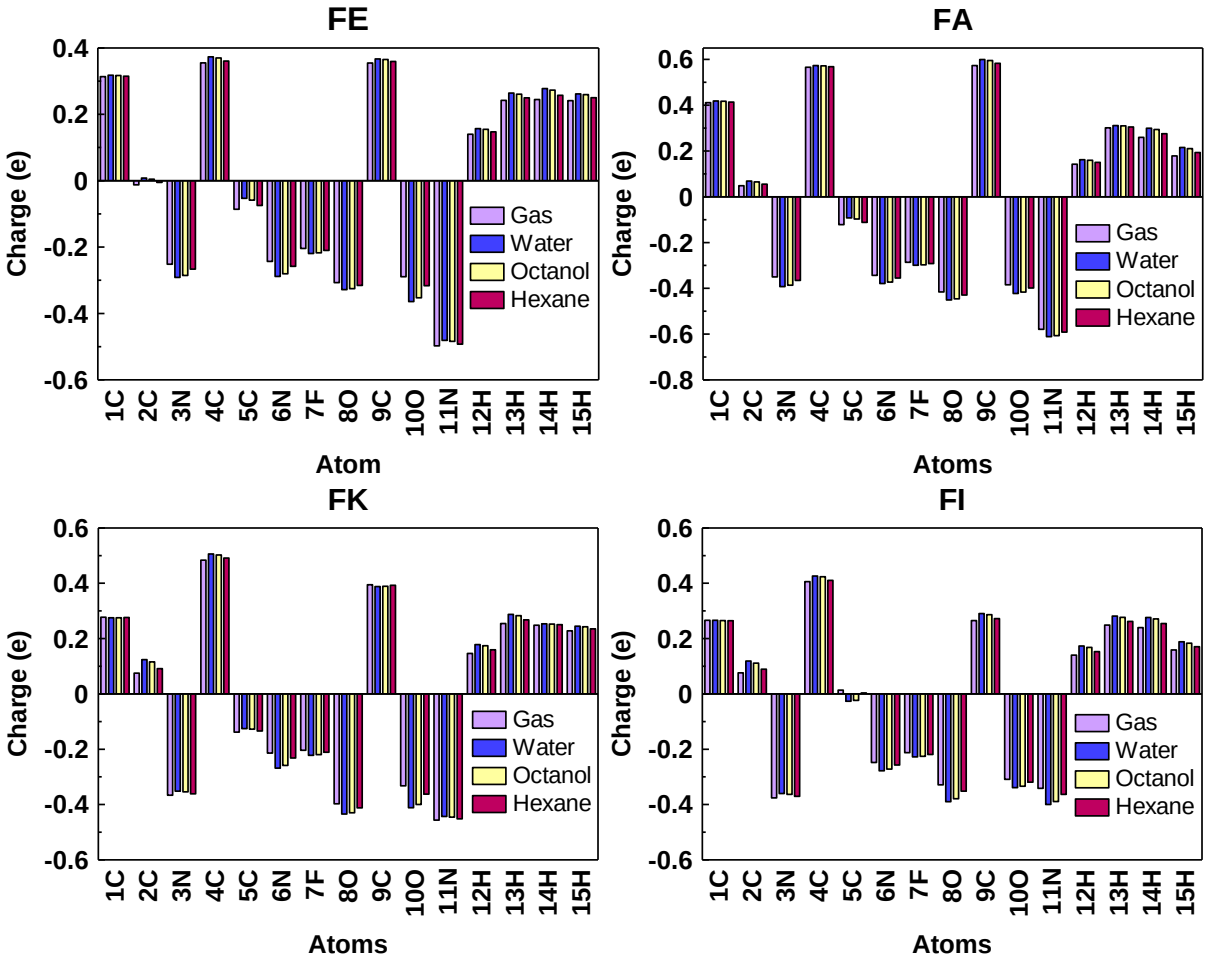

Figure 7. Atomic charges for favipiravir and its tautomers in gas and different solvents.

2.9 Molecular Electrostatic Potentials (MEP) surfaces

Molecular electrostatic potential (MEP) surfaces display the possible interaction sites of the studied molecules (Figure 8). The surface of the MEP is colour coded to show the density variations. The regions susceptible to nuclear and electrophile attacks are blue-coded (positive charged) and red (negative charged). The density of charges on MEP surfaces corresponds to the cargo distribution in Figure 6.The electrophilic region lies in the amine carboxamide group for all molecules. However, the nucleophilic area spreads to the group of hydroxyls via carbonyl oxygen, hydroxyl oxygen, and pyrazine ring nitrogen (N6). The N6 nucleophilic nitrogen atom represents a possible protonation site, particularly in biologically active environments for these molecules. Pyrazine is the site of potential contact between the molecules.

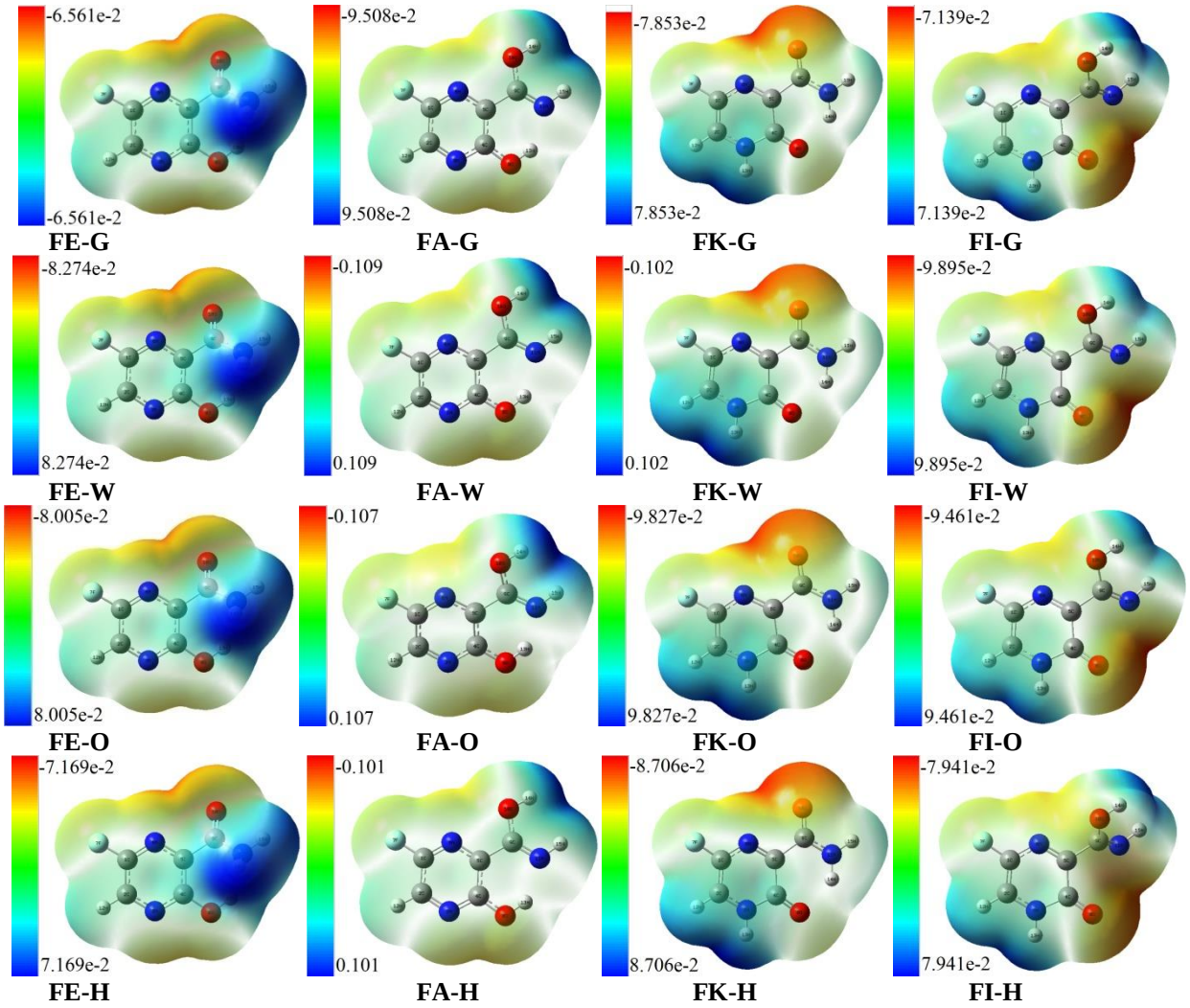

Figure 8. Molecular electrostatic potential energy surface (MEP) of favipiravir and its tautomers.

2.10 Docking Results

The docking procedure was made with the executable command from Autodock_Vina, which generated the structural poses for the rigid docking with the 6LU7 protein complex under affinity-based ranking around -5.6 Kcal/mol. However, as the binding pocket size was kept at 20 Å units, the affinity binding lost its ability to bind perfectly to generate less energy between -5.0 to -6.0 Kcal/mol, as shown in Table 6.

Table 6: Affinity calculations between ligand-receptor interactions

Ligand	**Affinity (Kcal/mol)**
Amide	-5.6
Enol	-5.4
Imidic	-5.2
Keto	-5.1

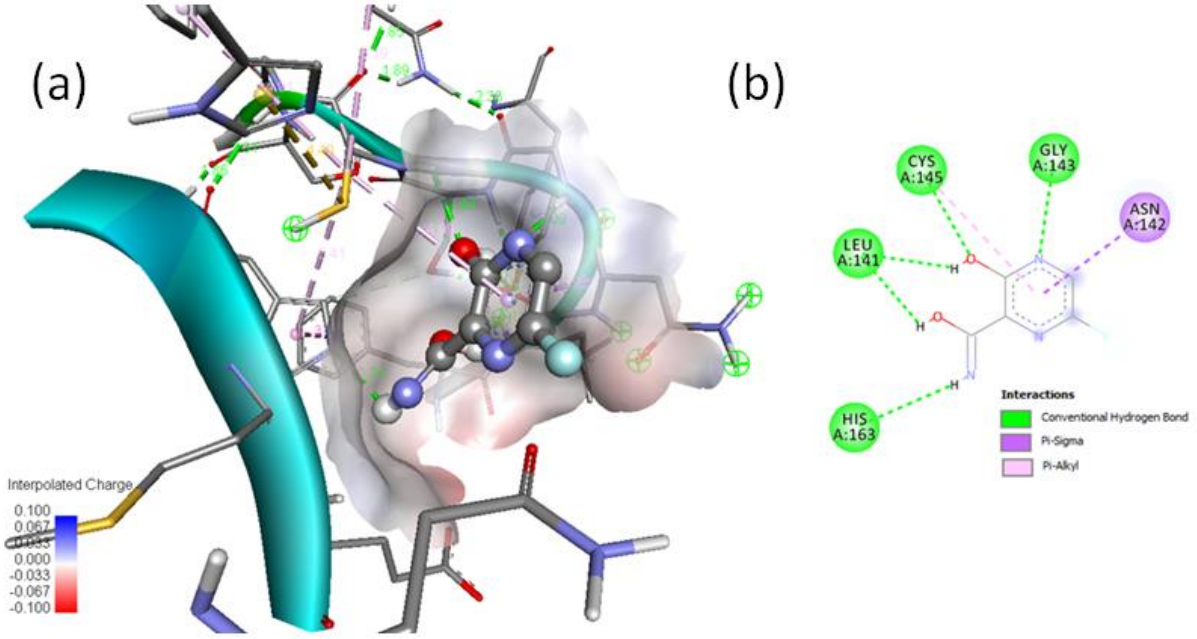

Figure 9. Molecular docking of 6LU7 Protease enzyme with active site bind favipiravir amide tautomer (a) Insight of binding interactions in 3D (b) Insight of binding interactions in 2D

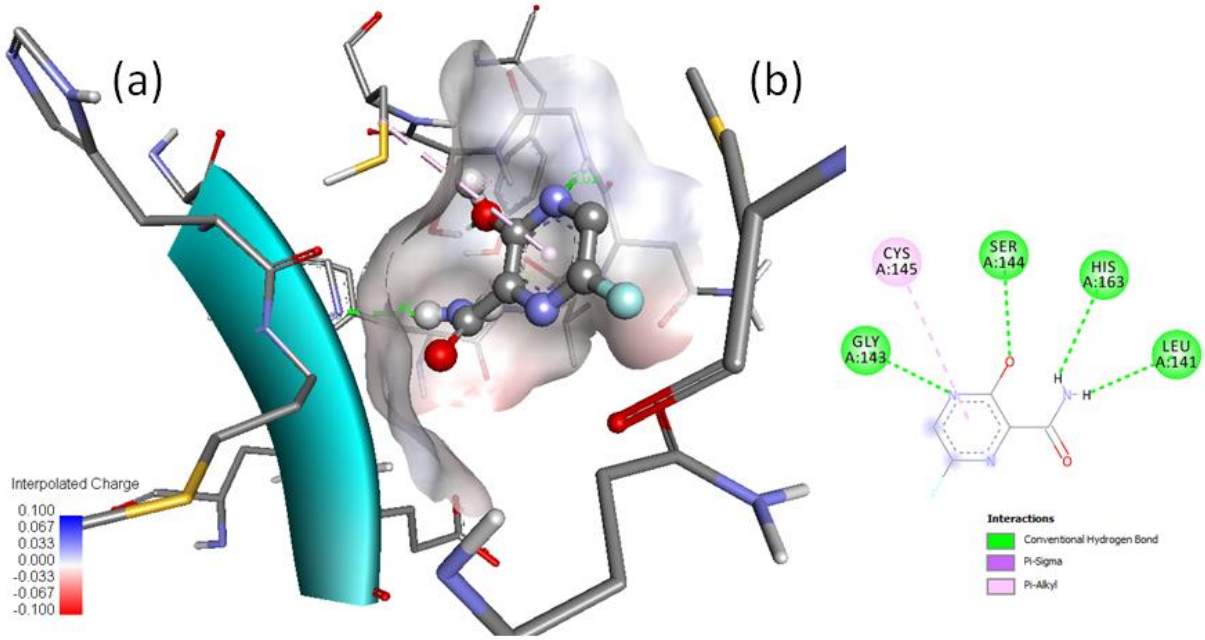

Figure 10. Molecular docking of 6LU7 Protease enzyme with active site bind favipiravir enol tautomer (a) Insight of binding interactions in 3D (b) Insight of binding interactions in 2D.

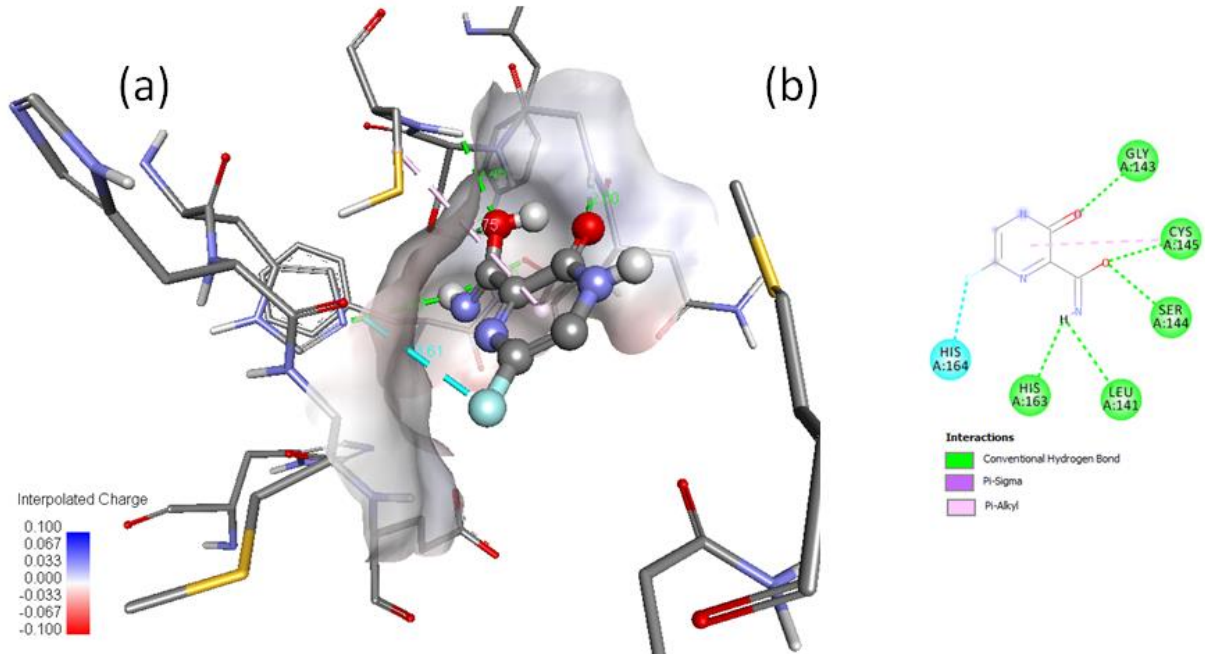

Figure 11. Molecular docking of 6LU7 Protease enzyme with active site bind favipiravir imidie tautomer (a) Insight of binding interactions in 3D (b) Insight of binding interactions in 2D

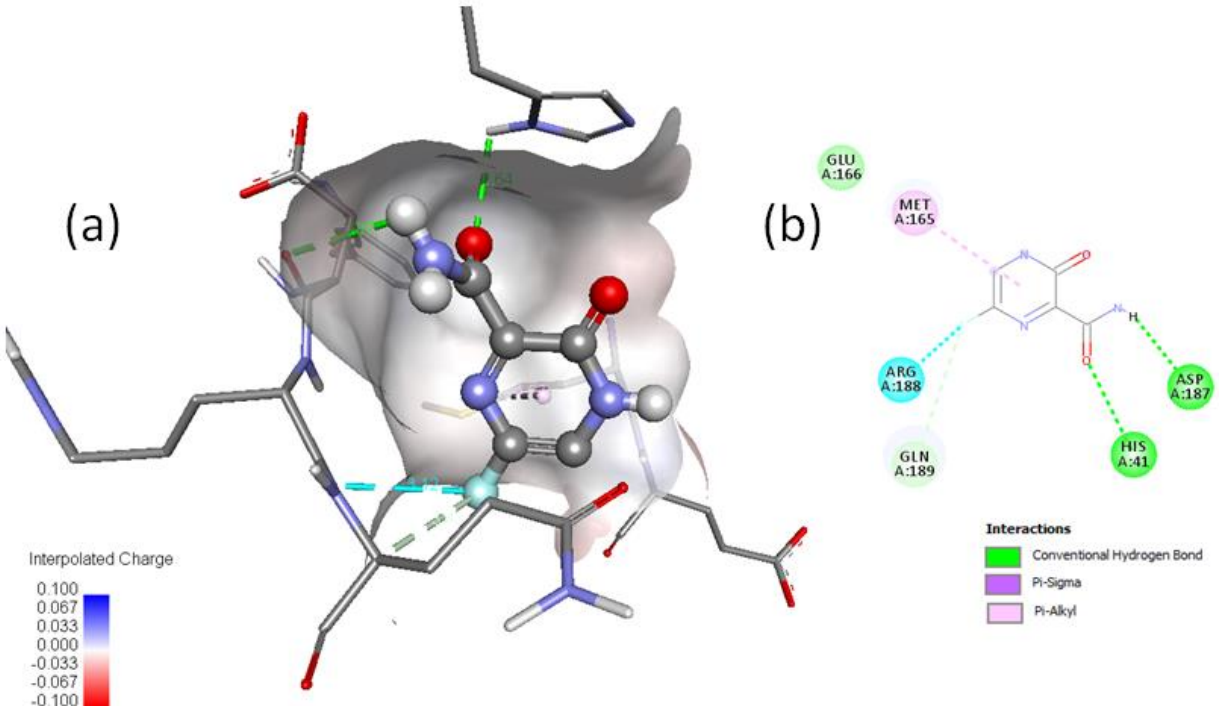

Figure 12. Molecular docking of 6LU7 Protease enzyme with active site bind favipiravir keto tautomer (a) Insight of binding interactions in 3D (b) Insight of binding interactions in 2D.

Considering the observations from the previous docking, results show that our study had effectively presented the binding of the tautomer active form of favipiravir in amide form in the active pocket as per the coordinates provided in the protocol.[77] The ligand molecules in the amide bond found to interact with the amino acid units highly include LEU141, GLY143, SER144, CYS145 and HIS163 in chain A of 6LU7 with hydrogen bonding with the functional groups of the ligand favipiravir amide form have –NH (side groups and ring groups) and –OH groups which were shown in figure 1. Compared to the other isomeric forms of the favipiravir, the amide bond shows

high affinity due to its free availability of two sets of –OH groups than the rest of the other forms. In overall observations from Figures 9 to Figure 12, the active site shows typically high reactivity with the LEU141 and GLY143 amino acids in the amide, enol and imidic form, where there is some steric interference shown in keto form towards the above amino acids to accept hydrogen bonding from ASP187 and HIS41 of the chain A.

Conclusion

The usefulness of global descriptors of reactivity, namely electrophilicity, chemical hardness, chemical potential (μ), electrophilicide index (to), softness (S), nucleofugality and electric fluid, reactivity prediction value of Favipiravir tautomers, were measured to determine the deal of the reactivity of HOMO and LUMO energy. Furthermore, the use of three solvents, water, octanol, and hexane, is studied in the solvent effect of molecules. The values obtained by FA tautomers display a lower value, and one can assume that FA can participate more in electrophile reactions than other tautomers in all phases. Furthermore, the operation of amide-form favipiravir has a higher binding affinity with 6LU7 in the overall docking procedure compared to the other tautomer forms.

REFERENCES

1. FurutaY, TakahashiK, FukudaYet al.In vitro and invivo Activities of Anti-Influenza Virus compound T-705. Antimicrob Agents Chemother.2002;46(4):977-981.
2. KisoM, TakahashiK, Sakai-TagawaYet al.T-705 (favipiravir) activityagainstlethal H5N1 influenza A viruses. ProcNatlAcadSci U S A.2010;107(2):882-887.
3. Gowen BB, Wong MH, Jung KH, Smee DF, Morrey JD, FurutaY. Efficacy of favipiravir (T-705) and T-1106 pyrazinederivatives in Phlebovirusdiseasemodels. Antiviral Res.2010;86(2):121-127.
4. Morrey JD, Taro BS, SiddharthanVet al.Efficacy of orallyadministered T-705 pyrazineanalog on lethalwestNilevirusinfection in rodents. Antiviral Res.2008;80(3):377-379.
5. Rocha-PereiraJ, JochmansD, DallmeierK, LeyssenP, Nascimento MS, NeytsJ. Favipiravir (T-705) inhibitsinvitroNorovirusreplication. BiochemBiophysResCommun.2012;424(4):777-780.
6. YamadaK, NoguchiK, KomenoT, FurutaY, NishizonoA. Efficacy of favipiravir (T-705) in rabiespostexposureprophylaxis. JInfectDis.2016;213(8):1253-1261.
7. Gowen BB, Wong MH, Jung KHet al.In vitro and invivoactivities of T-705 againstarenavirus and bunyavirusinfections. Antimicrob Agents Chemother.2007;51(9):3168-3176.
8. OestereichL, LüdtkeA, WurrS, RiegerT, Muñoz-FontelaC, GüntherS. Successful treatment of advanced Ebola virusinfection with T-705 (favipiravir) in a smallanimalmodel. Antiviral Res.2014;105:17-21.
9. FurutaY, TakahashiK, ShirakiKet al.T-705 (favipiravir) and relatedcompounds: novelbroad-spectruminhibitors of RNAviralinfections. Antiviral Res.2009;82(3):95-102.
10. ZhangT, ZhaiM, JiJ, ZhangJ, TianY, LiuX. Recent progress on the treatment of Ebola virusdisease with favipiravir and otherrelatedstrategies. BioorgMedChemLett.2017;27(11):2364-2368.
11. FurutaY, TakahashiK, inventors; Toyama Chemical Co., Ltd., assignee. Nitrogenous heterocyclic carboxamide derivatives or salts thereof and antiviral agents containing both. CA2339272A1. 2000.
12. ZhangT, KongL, LiZ, Yuan H-Y, Xu W-F. Synthesis of favipiravir. ChinJPharm.2013;44:841-844.
13. ShiF, LiZ, KongL, XieY, ZhangT, XuW. Synthesis and Crystal Structure of 6-fluoro-3-hydroxypyrazine-2-carboxamide. Drug DiscovTher.2014;8(3):117-120.
14. WanW, Min L-I-U, Xin-rongX, Qiu-YunDAI. Synthesis of favipiravir. JIntPharmRes.2015;42:220-224.
15. LiuF-L, LiC-Q, XiangH-Y, FengS. A practical and step-economicroute to favipiravir. ChemPap.2017;71(11):2153-2158.
16. ChenC, ZhangY, HuangJet al.Favipiravirversus Arbidol for COVID-19: A Randomized Clinical Trial; medRxiv[preprint]. InfectDis(except HIV/AIDS) **2020**, DOI:10.1101/2020.03.17.20037432.
17. DongL, HuS, GaoJ. Discovering Drugs to Treatcoronavirusdisease 2019 (COVID-19). Drug DiscovTher.2020;14(1):58-60.
18. AgrawalU, RajuR, Udwadia ZF. Favipiravir: Anew and emergingantiviraloption in COVID-19. MedJ Armed Forces India.2020;76(4):370-376.
19. Du YX, Chen XP. Favipiravir: pharmacokinetics and concernsaboutclinicaltrials for 2019-nCoV infection. ClinPharmacolTher.2020;108(2):242-247.
20. McKee DL, SternbergA, StangeU, LauferS, NaujokatC. Candidate drugsagainstSARS-CoV-2 and COVID-19. PharmacolRes.2020;157:104859.
21. ZhangJ, XieB, HashimotoK. Current status of potentialtherapeuticcandidates for the COVID-19 crisis. Brain BehavImmun.2020;87:59-73.
22. ZhangY, XuQ, SunZ, ZhouL. Current Targeted Therapeutics against COVID-19: based on first-lineexperience in China. PharmacolRes.2020;157:104854.
23. LiuC, ZhouQ, LiYet al.Research and Development on therapeuticagents and vaccines for COVID-19 and relatedhumancoronavirusdiseases. ACSCentSci.2020;6(3):315-331.
24. KhambholjaK, AsudaniD. Potential repurposing of favipiravir in COVID-19 outbreakbased on currentevidence. Travel MedInfectDis.2020;35:101710.

25. Jean SS, Lee PI, Hsueh PR. Treatment options for COVID-19: thereality and challenges. JMicrobiolImmunolInfect.2020;53(3):436-443.
26. Rabie AM, Cyanorona-20: The first potent anti-SARS-CoV-2 agent.International Immunopharmacology.2021,98,107831.
27. Rabie AM, Discovery of (E)-N-(4-cyanobenzylidene)-6-fuoro-3-hydroxypyrazine- 2-carboxamide (cyanorona-20): the first potent and specifc anti-COVID-19 drug.Chemical Papers (2021) 75:4669–4685.
28. FurutaY, KomenoT, NakamuraT. Favipiravir (T-705), a broadspectruminhibitor of viralRNA polymerase. Proc Jpn Acad Ser B Phys Biol Sci.2017;93(7):449-463.
29. WangM, CaoR, ZhangLet al.Remdesivir and chloroquineeffectivelyinhibit the recentlyemergednovelcoronavirus (2019-nCoV) invitro. Cell Res.2020;30(3):269-271.
30. Smither SJ, Eastaugh LS, Steward JA, NelsonM, Lenk RP, Lever MS. Post-exposureefficacy of oral T-705 (favipiravir) againstinhalational Ebola virusinfection in a mousemodel. Antiviral Res.2014;104:153-155.
31. SissokoD, LaouenanC, FolkessonEet al.Réné Lolamou; Loua C.-M.; Massala:V.; Moumouni, K.; Provost, C.; Samake, N.; Sekou, C.; Soumah, A.; Arnould, I.; Komano, M. -S.; Gustin, L.; Berutto, C.; Camara, D.; Camara, F. -S.; Colpaert, J.; Delamou, L.; Jansson, L.; Kourouma, E.; Loua, M.; Malme, K.; Manfrin, E.; Maomou, A.; Milinouno, A.; Ombelet, S.; Sidiboun, A. -Y.; Verreckt, I.; Yombouno, P.; Bocquin, A.; Carbonnelle, C.; Carmoi, T.; Frange, P.; Mely, S.; Nguyen, V. -K.; Pannetier, D.; Taburet, A. -M.; Treluyer, J. -M.; Kolie, J.; Moh, R.; Gonzalez, M. -C.; Kuisma, E.; Liedigk, B.; Ngabo, D.; Rudolf, M.; Thom, R.; Kerber, R.; Gabriel, M.; Di Caro, A.; Wölfel, R.; Badir, J.; Bentahir, M.; Deccache, Y.; Dumont, C.; Durant, J. -F.; El Bakkouri, K.; Gasasira Uwamahoro, M.; Smits, B.; Toufik, N.; Van Cauwenberghe, S.; Ezzedine, K.; D'Ortenzio, E.; Pizarro, L.; Etienne, A.; Guedj, J.; Fizet, A.; Barte de Sainte Fare, E.; Murgue, B.; Tran-Minh, T.; Rapp, C.; Piguet, P.; Poncin, M.; Draguez, B.; Allaford Duverger, T.; Barbe, S.; Baret, G.; Defourny, I.; Carroll, M.; Raoul, H.; Augier, A.; Eholie, S. P.; Yazdanpanah, Y.; Levy-Marchal, C.; Antierrens, A.; Van Herp, M.; Günther, S.; de Lamballerie, X.; Keïta, S.; Mentre, F.; Anglaret, X.; Malvy, D.; JIKI Study Group Experimental Treatment with Favipiravir for Ebola Virus Disease (the JIKI Trial): A Historically Controlled, Single-Arm Proof-of-Concept Trial in Guinea. PLOS Med.**2016,** 13 (3), e1001967.
32. Bai CQ, Mu JS, KargboDet al.Clinical and virologicalcharacteristics of Ebola virusdiseasepatientstreated with favipiravir (T-705)-Sierra Leone, 2014. ClinInfectDis.2016;63(10):1288-1294.
33. YaraghiA, Ozkendir O-M, MirzaeiM. DFTstudies of 5-fluorouraciltautomers on a silicongraphenenanosheet. Superlat.microstruct.2015;85:784-788.
34. NaderiE, MirzaeiM, SaghaieL, KhodarahmiG, GulserenO. Relaxations of Methylpyridinone tautomers at the C60 surfaces: DFTstudies. IntJ Nano Dimens.2017;8:124-131.
35. KouchakiA, GülserenO, HadipourN, MirzaeiM. Relaxations of fluorouraciltautomers by decorations of fullerene-likeSiCs: DFTstudies. PhysLett A.2016;380(25-26):2160-2166.
36. Abyar GhamsariP, SamadizadehM, MirzaeiM. Cytidine derivatives as inhibitors of methyltransferaseenzyme. Eurasian ChemCommun.2020;2(4):433-439.
37. Ghanadzadeh GilaniA, TaghvaeiV, Moradi RufchahiE, MirzaeiM. Tautomerism, solvatochromism, preferentialsolvation, and densityfunctionalstudy of some Heteroarylazo dyes. JMolLiq.2019;273:392-407.
38. SoleimaniM, MirzaeiM, MofidM-R, KhodarahmiG, RahimpourS-F. Lactoperoxidase inhibition by tautomericpropylthiouracils. AsianJ.Green Chem.2020;4:1-10.
39. MirzaeiM, Hadipour NL, AhmadiK. Investigation of C-H …O=C and N-H …OChydrogen-bondinginteractions in crystallinethymine by DFTcalculations of O-17, N-14 and H-2 NQRparameters. BiophysChem.2007;125(2-3):411-415.
40. NazemiH, MirzaeiM, JafariE. Antidepressant activity of curcumin by monoamine oxidase–A inhibitionAdv. JChem B.2019;1(1):3-9.
41. CartaA, BriguglioI, PirasSet al.A combinedinsilico/invitroapproachunveilscommonmolecularrequirements for efficientBVDVRdRpbinding of lineararomatic N-polycyclicsystems. EurJMedChem.2016;117:321-334.
42. Frisch M-J, Trucks G-W, SchlegelHBet al.Gaussian. GaussianInc Wallingford Conn SA.2009;09, RevisionA.1.
43. Becke AD. Density-functionalthermochemistry. III. The role of exactexchange. ChemPhys.1993;98(7):5648-5652.
44. LeeC, YangW, Parr RG. Development of the Colle-Salvetticorrelation-energyformula into a functional of the electrondensity. PhysRev B Condens Matter.1988;37(2):785-789.
45. Stephens PJ, Devlin FJ, Chabalowski CF, Frisch MJ. Ab Initio calculation of vibrationalabsorption and circular dichroismspectrausingdensityfunctionalforce fields. JPhysChem.1994;98(45):11623-11627.
46. DenningtonR, Keith T-M-J. GaussView.USA: GaussianInc, 2009.
47. TomasiJ, MennucciB, CammiR. Quantum mechanicalcontinuumsolvationmodels. ChemRev.2005;105(8):2999-3093, DOI:10.1021/cr9904009.
48. RCSB, PDB.Protein Data Bank;2005.

49. GuexN, Peitsch MC. SWISS-MODEL and the Swiss-Pdb viewer: anenvironment for comparativeproteinmodeling. Electrophoresis.1997;18(15):2714-2723.
50. Studio, Discovery Studio Accelrys**2008**; vol 2(1).
51. Wishart DS, Feunang YD, Guo ACet al.DrugBank 5.0: A majorupdate to the DrugBank database for 2018. Nucleic Acids Res.2018;46(D1):D1074-D1082.
52. UltraCD. 6.0 and Chem3D Ultra.Cambridge: Cambridge Soft Corporation;2001.
53. ForliS, HueyR, Pique ME, Sanner MF, Goodsell DS, Olson AJ. Computational protein–liganddocking and virtualdrugscreening with the AutoDock suite. NatProtoc.2016;11(5):905-919.
54. Adeniyi AA, Ajibade PA. Comparing the suitability of autodock, gold and glide for the docking and predicting the possibletargets of Ru(II)-basedcomplexes as anticanceragents. Molecules.2013;18(4):3760-3778.
55. TrottO, Olson A-J, VinaAD.Improving the speed and accuracy of docking with a newscoringfunction, efficientoptimization, and multithreading. JComputChem.2009:NA-NA.
56. DeLano W-L;2002. Physiology molv0.99. DeLano.San Carlos, CA: Scientific:700.
57. Joshi BD, Chaudhary MK. NBO, nonlinear optical and thermodynamicproperties of 10-acetyl-10H-phenothiazine 5-oxide. BIBECHANA.2018;15:131-139.
58. Joshi BD, MishraR, TandonP, OliveiraAC, AyalaAP. Quantum chemicalstudies of structural, vibrational, NBO and hyperpolarizability of ondansetron hydrochloride. JMolStruct.2014;1058:31-40.
59. Bevan OttJ, Boerio-GoatesJ. Chemical Thermodynamics: Principles and Applications.San Diego, (CA): Academic Press;2000.
60. PengC, Ayala PY, Schlegel HB, Frisch MJ. Using redundantinternalcoordinates to optimizeequilibriumgeometries and transitionstates. JComputChem.1996;17(1):49-56.
61. AssomaA, BenjamineBedeL, A, KoneM, N'GussanY. Thomas. Theoretical study of stability, tautomerism, equilibriumconstants (pK^T), activationenergies and acidity of 6-thioxanthine in gasphase by the abinitiomethod and functionaldensitytheorycalculationsEuropenJ. SciRes.2010;44(2):337-354.
62. KarelsonM. Molecular Descriptors in QSAR/QSPR.New York: John Wiley & Sons;2000.
63. ZhouZ. Pan-, R.G. Activation Hardness: New Index for Describing the Orientation of Electrophilic Aromatic Substitution. JAmChemSoc.1990;772(15):5720-5724.
64. ParrRG, Szentpály Lv, LiuS. Electrophilicity index. JAmChemSoc.1999;121(9):1922-1924.
65. ChattarajPK, GiriS. Stability, reactivity, and aromaticity of compounds of a multivalentsuperatom. JPhysChem A.2007;111(43):11116-11121.
66. RoosG, LoverixS, BrosensEet al.The activation of electrophile, nucleophile and Leaving Group during the reactioncatalysed by pI258 arsenate reductase. ChemBioChem.2006;7(6):981-989.
67. CorredorC, TeslovaT, Cañamares MVet al.M.Raman and surface-enhancedRamanspectra of chrysin, apigenin and luteolin. VibSpectrosc.2009;49(2):190-195.
68. Young RJ, Green DV, Luscombe CN, Hill AP. Getting physical in drugdiscovery II: The impact of chromatographichydrophobicitymeasurements and aromaticity. Drug Discov Today.2011;16(17-18):822-830.
69. ZhangJ, TuguldurB, van der SpoelD. Force fieldbenchmark of organicliquids. 2. Gibbsenergy of solvation. JChemInfModel.2015;55(6):1192-1201.
70. Mobley DL, Wymer KL, Lim NM, Guthrie JP. Blind prediction of solvationFreeenergies from the SAMPL4 challenge. JComputAidMolDes.2014;28(3):135-150.
71. ShivakumarD, HarderE, DammW, Friesner RA, ShermanW. Improving the prediction of absolutesolvationFreeenergiesusing the nextgenerationOPLSforce field. JChemTheorComput.2012;8(8):2553-2558.
72. Fennell CJ, Wymer KL, Mobley DL. A Fixed-chargemodel for alcoholpolarization in the condensedphase, and itsrole in smallmoleculehydration. JPhysChem B.2014;118(24):6438-6446.
73. OostenbrinkC, VillaA, Mark AE, van GunsterenWF. A Biomolecular Force Field Based on the Free Enthalpy of Hydration and Solvation: theGROMOS Force-Field Parameter sets 53A5 and 53A6. JComputChem.2004;25(13):1656-1676.
74. LiaoQ, YaoJ, YuanS. Concepts in biochemicalpharmacology: Part 1.Mol. DiversKeenP, BrodieBB, GilletteJR, AckermanHS, eds.; vol10(3), 301. 78.Heidelberg: Springer;1971, **2006**:213.
75. HanschC, Björkroth JP, LeoA. Hydrophobicity and centralnervoussystemagents: on the principle of minimalhydrophobicity in drugdesign. JPharmSci.1987;76(9):663-687.
76. ShargelL, YuA, Wu-PongS.Applied Biopharmaceutics and Pharmacokinetics.6th ed.New York: McGraw-Hill Education;2012.
77. Rhyman, Lydia, MahirTursun H-H, CemalParlakAYSC, KharkarP,RamasamiP. Theoretical investigation of the derivatives of favipiravir (T-705).AsPotentialDrugs for Ebola VirusPhysical Sciences Reviews 3, No.92018.